Pre-screening the intrinsic angiogenic capacity of biomaterials in an optimised *ex ovo* chorioallantoic membrane model

Nupur Kohli[1,2] (iD), Prasad Sawadkar[1], Sonia Ho[1], Vaibhav Sharma[1], Martyn Snow[3], Sean Powell[4], Maria A Woodruff[4], Lilian Hook[5] and Elena García-Gareta[1]

Abstract

Biomaterial development for clinical applications is currently on the rise. This necessitates adequate *in vitro* testing, where the structure and composition of biomaterials must be specifically tailored to withstand *in situ* repair and regeneration responses for a successful clinical outcome. The chorioallantoic membrane of chicken embryos has been previously used to study angiogenesis, a prerequisite for most tissue repair and regeneration. In this study, we report an optimised *ex ovo* method using a glass-cling film set-up that yields increased embryo survival rates and has an improved protocol for harvesting biomaterials. Furthermore, we used this method to examine the intrinsic angiogenic capacity of a variety of biomaterials categorised as natural, synthetic, natural/synthetic and natural/natural composites with varying porosities. We detected significant differences in biomaterials' angiogenesis with natural polymers and polymers with a high overall porosity showing a greater vascularisation compared to synthetic polymers. Therefore, our proposed *ex ovo* chorioallantoic membrane method can be effectively used to pre-screen biomaterials intended for clinical application.

Introduction

Adequate *in vitro* biomaterial testing is vital for predicting the success of a biomaterial *in vivo*. Therefore, a significant amount of research is underway to screen biomaterials prior to pre-clinical *in vivo* animal testing, which is considered a prerequisite for clinical studies.[1,2] It is well established that significant inconsistencies exist between predicted outcomes of biomaterials tested *in vitro* and their actual performance *in vivo*. A focus of current research is to establish models that could bridge the gap between *in vitro* testing and *in vivo* outcomes in accordance with the principles of NC3Rs (National Committee for Reduction, Refinement and Replacement of Animals).

Recently, chorioallantoic membrane (CAM) assays of the chick embryo are gaining wide popularity as they are a cost-effective and less sentient '*in vivo*' model for biomaterial

testing.[3] The primary reason for this is that the CAM is highly vascularised, constituting both mature vessels and capillaries, and is easily accessible for orthotopic implantation of biomaterials without initiating an immune reaction from the

[1]Regenerative Biomaterials Group, RAFT Institute, Mount Vernon Hospital, Northwood, UK
[2]Department of Mechanical Engineering, Imperial College London, London, UK
[3]Royal Orthopaedic Hospital NHS Foundation Trust, Birmingham, UK
[4]Institute of Health and Biomedical Innovation, Queensland University of Technology, Brisbane, Australia
[5]Smart Matrix Limited, Leopold Muller Building, Mount Vernon Hospital, Northwood, UK

Corresponding author:
Nupur Kohli, Department of Mechanical Engineering, Imperial College London, South Kensington Campus, London SW7 2AZ, UK.
Email: n.kohli@imperial.ac.uk

developing embryo. The gestation period of a chick embryo is 21 days, with the CAM formed around embryonic day (ED) 4 following the fusion of the allantois and the chorion membrane. The function of this membrane is to provide gaseous exchange between the developing embryo and the eggshell pores, and allow ion and nutrient exchange.[4] The capillary bed of the CAM is non-innervated and has been used in the field of tissue engineering for over four decades to study graft versus host reactions.[5,6]

In 2006, the US Food and Drug Administration (FDA) approved CAM models for pre-clinical evaluation of products used for the treatment of chronic cutaneous wounds.[7] More recently, CAMs have been used to perform anti-angiogenic studies in cancer research and for assessing the angiogenic behaviour of biomaterials under development for tissue engineering applications.[8,9] CAMs can be used in an *in ovo* or *ex ovo* form for studying angiogenesis.[10–13] *In ovo* CAM assays are very popular, but due to the lack of standardisation, a significant amount of variation exists in the technique. Moreover, the *in ovo* approach is inefficient in maintaining sterility and often results in contamination from the eggshell dust. Recent advancements in *ex ovo* culture techniques have resulted in the development of an efficient, reproducible, and cost-effective assay that is slowly gaining popularity for testing angiogenesis in biomaterials.[13,14]

A wide variety of biomaterials with different structures and compositions are being developed at a rapid pace to address various unmet clinical needs. Varying structure and composition can have a large effect on function – at the extremes resulting in successful outcomes with tissue repair and regeneration or in failed outcomes with no tissue repair or biomaterial rejection.[15,16] Critical to the repair process in many therapeutic applications is the restoration of blood vessels, to supply nutrients and oxygen to the damaged tissue. The porous structure of a biomaterial plays a key role in biomaterial revascularisation. However, the extent to which other parameters, such as composition and mechanical properties, also affect biomaterial revascularisation is still not clear.[16,17] Composition here refers to the material the scaffold is composed of and not its surface roughness, crystallinity and surface energy. Oates et al, utilised the *in ovo* CAM assays to demonstrate how specific material characteristics such as porosity and pore size could affect a biomaterial's intrinsic angiogenic potential.[18] Other studies have also shown that changing the structure and composition of a biomaterial directly affects its angiogenic potential, for example, crosslinked collagen matrices with a high average pore size and a rigid structure show a significantly higher angiogenic potential compared to non-crosslinked polymers.[19,20] The chemical composition of smooth materials such as Tecoflex®, which is a medical-grade aliphatic polyether polyurethane and polyvinylchloride (PVC), has previously been shown to induce an anti-angiogenic response,

whereas rough materials such as filter paper and collagen/elastin membranes have been shown to induce an angiogenic response.[10] These studies suggest that the extent of angiogenic response of a biomaterial *in vivo* is dependent on multiple factors but mainly depends on porosity and the composition. Therefore, it is vital to pre-screen biomaterials under development using methods that mimic the *in vivo* situation as closely as possible.

While the *in ovo* CAM assay is popular, only a handful of studies have used the *ex ovo* method for biomaterial testing.[3,13,21–23] The aims of this study were (1) to optimise the previously reported *ex ovo* CAM assays using a glass-cling film set-up and (2) to report the suitability of this method in screening biomaterials to select candidates for further development by examining the angiogenic capacity of a range of biomaterials.

Materials and methods

Fabrication of biomaterials

Biomaterials used in this study were categorised as natural, synthetic, natural/synthetic and natural/natural (Figure 1). These were (Table 1) (1) three-dimensional (3D) porous collagen matrix, fabricated using 90% collagen type I (FirstLink, Wolverhampton, UK) and 10% Minimum Essential Medium (MEM; Invitrogen, Paisley, UK). This solution was neutralised by 5 M NaOH and crosslinked with 0.25% glutaraldehyde; (2) 3D crosslinked porous matrix of bovine fibrin, fabricated using 2% bovine fibrinogen in phosphate-buffered saline (PBS) and 10% thrombin, crosslinked with 0.25% glutaraldehyde; (3) 3D crosslinked porous matrix of elastin, fabricated from 10% (v/v) of the elastin powder (Sigma, Dorset, UK) mixed with 1 mL of 0.5 M oxalic acid (freshly prepared) at room temperature and crosslinked with 2.5% glutaraldehyde; (4) electrospun poly-ε-caprolactone (PCL), commercially purchased from The Electrospinning Company Ltd. (Didcot, UK) (micro-PCL); (5) electrospun PCL, fabricated in Professor Maria A. Woodruff's lab using the methods described in Ristovski et al.[24] (macro-PCL); (6) silicone, purchased from BITY Mould Supply (Richardson, TX, USA); (7) commercially available dermal replacement scaffold Integra®, a 3D crosslinked porous matrix made of bovine tendon collagen type I with 10%–15% chondroitin-6-sulphate from shark cartilage and a silicone backing layer (Integra Life Science Corporation, Plainsboro, NJ, USA); (8) electrospun PCL and 3D porous matrix of bovine fibrin (PCL/Fib) composite scaffolds fabricated using micro-PCL and coated with fibrin; (9) electrospun PCL and collagen (PCL/Col) scaffold fabricated using micro-PCL and coated with neutralised collagen; (10) 3D crosslinked porous matrix made of bovine fibrin and alginate, developed in our laboratory; (11) commercially available dermal replacement scaffold Matriderm®, a 3D porous matrix of bovine collagen types I,
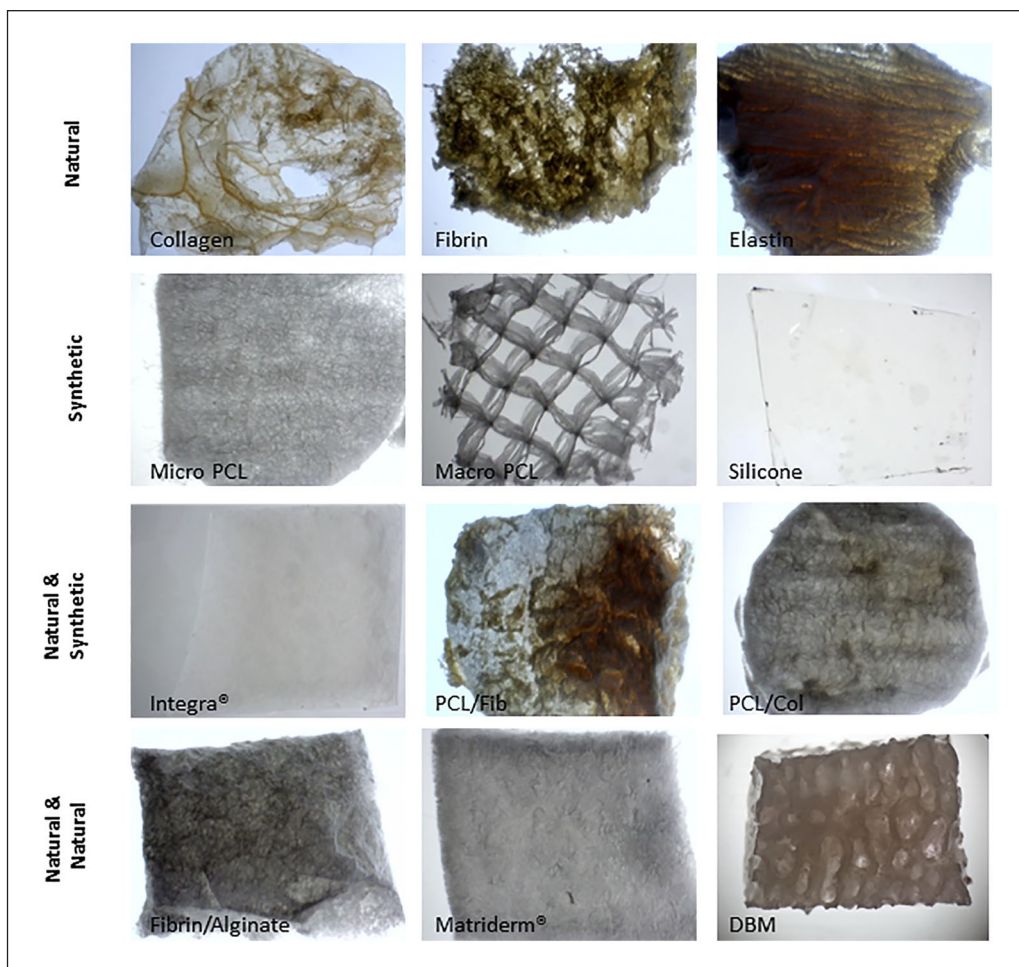
Figure 1. Representative stereo microscope images of the biomaterials tested. The stereo microscopic images show the overall structure of the biomaterials tested, highlighting the differences in their architecture. Macroscopically, each biomaterial appears intact and ranges in appearance from fibrous to porous matrices, except silicone which appears as a transparent sheet.

III and V, and elastin hydrolysate (MedSkin Solutions, Billerbeck, Germany); and (12) demineralised bone matrix (DBM) clinically available and supplied by NHS-BT (Birmingham, UK).

Scanning electron microscopy

Biomaterials were mounted on stubs and sputter-coated with carbon coater. All images were obtained using a secondary electron detector in a Philips XL 30 Field Emission scanning electron microscope, operated at 5 kV and an average working distance of 10 mm.

Porosity and pore size analyses

To calculate percentage porosity and pore size range of scaffolds, scanning electron microscopy (SEM) images were quantitatively analysed using ImageJ bundled with 64-bit Java 1.6.0 (National Institutes of Health (NIH), USA). A threshold frequency was adjusted to visualise all pores. An area fraction function was used for calculating porosity, and particle analysis function was used to determine the diameter of each pore. For porosity, $n = 3$ different scaffolds were used, except for scaffolds with porosity values previously reported in the literature (Integra®, fibrin/alginate and DBM). The previously published values may have been calculated using alternate methods of measuring porosity such as histology or mercury intrusion porosimetry. For pore size range, $n = 3$ different SEM images from three different scaffolds were used with over 1000 pores analysed per scaffold to determine the gradient pore structure (GPS) and the frequency of each pore diameter.

Ex ovo *experimental set-up*

We compared two methods in this study: previously published methods using weighing boats for the *ex ovo* set-up and our proposed method called the glass-cling film set-up. For details on the previously published methods, refer to the study by Dohle et al.[13]

Table 1. A summary of the biomaterials used in this study with their structural composition and functional properties.

Name	Composition	Application	Development phase
Collagen	Natural scaffold 3D crosslinked porous matrix of collagen type I from rat tail tendon	Soft tissue regeneration	Pre-clinical
Fibrin	Natural scaffold 3D crosslinked porous matrix of bovine fibrin	Soft tissue regeneration	Pre-clinical
Elastin	Natural scaffold 3D crosslinked porous matrix of elastin from bovine ligament	Soft tissue regeneration	Pre-clinical
Micro-PCL	Synthetic scaffold Electrospun PCL	Soft tissue regeneration	Pre-clinical
Macro-PCL	Synthetic scaffold Electrospun PCL	Bone regeneration	Pre-clinical
Silicone	Synthetic scaffold Platsil 73-15 Precision Silicone	Epidermal component of skin scaffolds	In clinical use
Integra®	Natural and synthetic composite scaffold 3D crosslinked porous matrix made of bovine tendon collagen type I with 10%–15% chondroitin-6-sulphate from shark cartilage and a silicone backing layer	Repair of full-thickness skin wounds	In clinical use
PCL/Fib	Natural and synthetic composite scaffold Electrospun PCL and 3D porous matrix of bovine fibrin	Soft tissue regeneration	Pre-clinical
PCL/Col	Natural and synthetic composite scaffold Electrospun PCL and 3D porous matrix of collagen type I from rat tail	Soft tissue regeneration	Pre-clinical
Fibrin/Alginate	Natural composite scaffold 3D crosslinked porous matrix made of bovine fibrin and alginate	Repair of full-thickness skin wounds	Pre-clinical
Matriderm®	Natural composite scaffold 3D porous matrix of bovine collagen types I, III and V, and elastin	Repair of full-thickness skin wounds	In clinical use
Demineralised bone matrix (DBM)	Type I collagen and non-collagenous proteins	Bone regeneration	In clinical use

3d: three-dimensional; PCL: poly-ε-caprolactone.

A glass-cling film set-up was used for maintaining the *ex ovo* cultures (Figure 2). Pyrex glasses of 8 cm diameter were autoclaved for sterilisation. The glasses were filled up to three-quarters with sterile water and a clean cling film layer (pre-sterilised with 70% industrial methylated spirit (IMS) and dried) was placed inside the glasses ensuring that the bottom of the cling film touched the water. Next, 500 μL of antibiotic, antimycotic solution (Sigma, Dorset, UK) was pipetted onto the cling film at a final concentration of 1 in 100. This solution is referred to as antimicrobial solution (AM solution) in this study. Rubber bands were used to secure the cling film on the glasses.

Ex ovo *CAM assays*

The use of chick embryos in this study did not require ethical approval as per the guidelines of the Institutional Animal Care and Use Committee (IACUC) and the NIH (USA), which states that a chick embryo that has not reached the 14th day of its gestation period would not experience pain and can therefore be used for experimentation without any ethical restrictions or prior protocol approval.[25,26] Fertile chicken eggs were purchased from local farms in Middlesex (UK) and incubated in an egg incubator with automatic rotation for 3 days at 38°C and 45%–50% humidity. At day 3, eggs were wiped with cytosol and cracked open using a triangle magnetic stirrer. The contents were immediately transferred to the glass-cling film set-up described above. The yolk sac and the embryo were identified and assessed for viability by looking for a beating heart. To prevent contamination from the egg shells, 500 μL of antimicrobial solution was pipetted gently onto the albumen. The glasses were then covered with a Petri dish and transferred to the incubator and grown for a further 6 days at 38°C and 80%-90% humidity. At day 9, up to six scaffolds (roughly 5 mm × 5 mm in size) were implanted on the CAM as shown in Figure 3. Filter discs soaked in vascular endothelial growth factor (VEGF) and PBS were used as positive and negative controls, respectively. After placement of the scaffolds, the *ex ovo* cultures were incubated for a further 3 days.
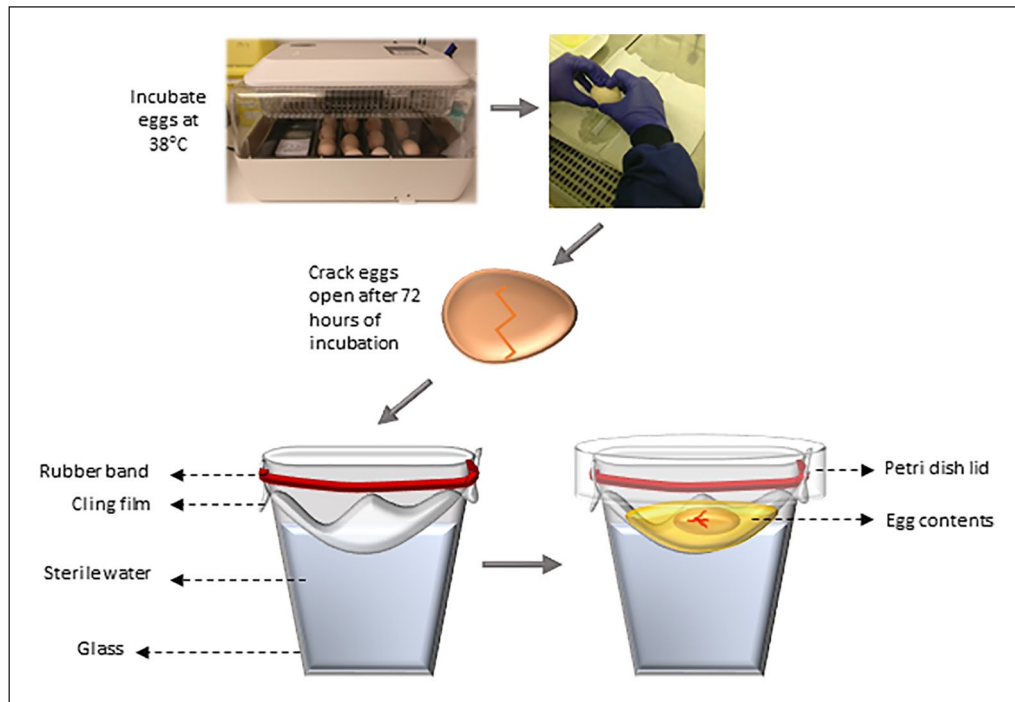
Figure 2. A pictorial illustration of *ex ovo* cultures. A step-by-step procedure is shown from incubating the eggs to culturing them *ex ovo*. The proposed glass-cling film set-up is shown detailing the materials required to successfully perform shell-less cultures.
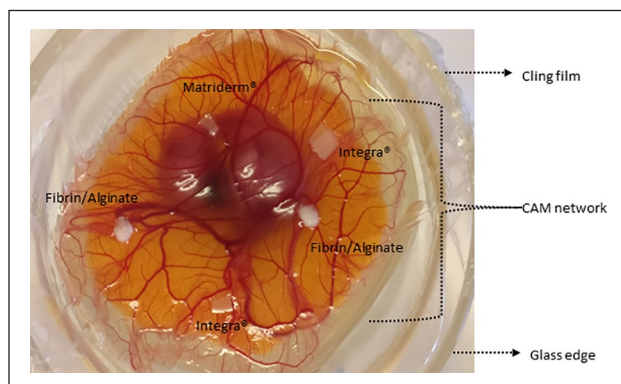

Figure 3. An example of biomaterial implantation on the CAM. The contents of the shell-less cultures are imaged from above, showing the embryo, the developing CAM and the different biomaterials at day 9.

CAM assay analyses

At the end of the testing period (ED 12), embryos were euthanised under the British Home Office regulations by freezing at −20°C for approximately 15 min. The CAM was then covered with 5 mL of 4% paraformaldehyde (PFA) for 15 min (to avoid bleeding of CAM after excision). The scaffolds were carefully dissected out with a 5-mm perimeter of the CAM excised along with the scaffold. Images were acquired by inverting the scaffolds to observe infiltrating blood vessels from underneath, using GT vision stereo microscope (GXM-XTL3T101) for

further analysis. After imaging, some excised scaffolds were prepared for histological sectioning and haematoxylin and eosin staining (H&E). Scaffolds were processed, embedded in paraffin wax and sectioned using a standard rotary microtome into 4-μm-thick sections. After de-paraffinising using xylene and rehydrating sections, slides were dipped in Shandon™ Gill™ Hematoxylin (Thermo Fisher Scientific, Loughborough, UK) for 10 min, followed by a warm tap water wash for another 10 min. Sections were then stained with Thermo Scientific™ Shandon™ Eosin Y Cytoplasmic counterstain (Thermo fisher scientific, Loughborough, UK) for 4 min followed by dehydration, clearing, and mounting with cover slips for imaging. Sections were imaged using 10× magnification and then stitched using Microsoft Image Composite Editor (ICE) software.

Quantification of vascularised scaffolds

Stereo microscope images of the scaffolds were processed using the 'vessel-analysis' plug-in, in the ImageJ software (NIH). Images were first automatically converted into binary images and then the vascular density analysis function was applied. The vascular density was calculated relative to the scaffold size since some biomaterials shrink by the end of the assay. The software automatically calculates the vascular density normalised to the area of the scaffold. Bifurcation points were counted in each image using ImageJ 'counter' function by digitally selecting the number
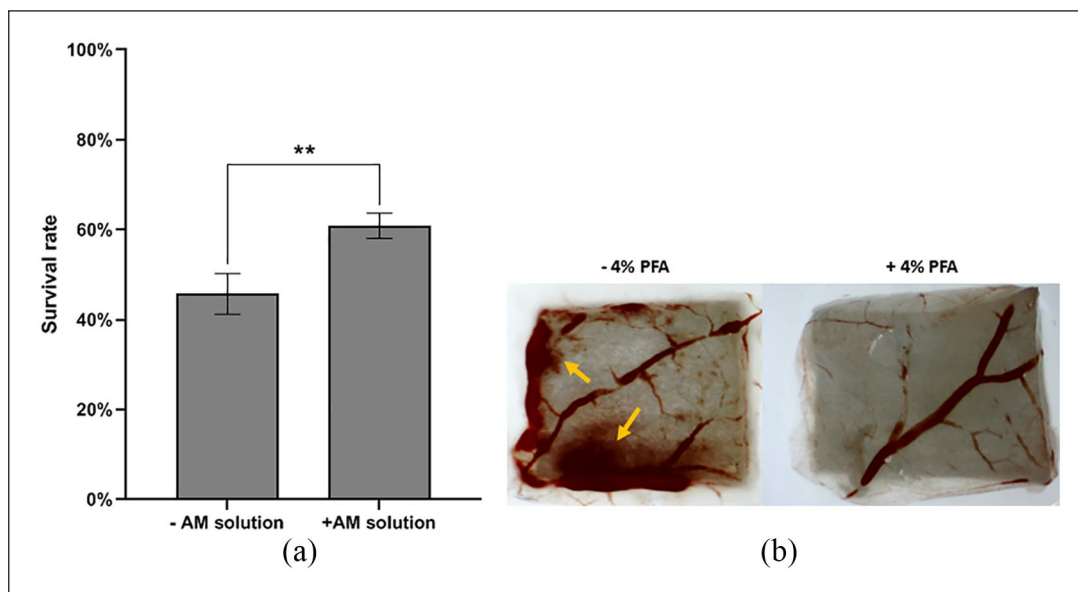
Figure 4. Data for optimised *ex ovo* method. (a) Survival rate of embryos using the new method (+AM solution) was significantly greater (*p* = 0.0093; unpaired *t*-test) than the previously published method (–AM solution). Data are presented as mean ± SE in each case. (b) Representative images are shown of micro-PCL biomaterial excised without fixation (–4% PFA) and with fixation (+4% PFA). Yellow arrows indicate the areas of excessive bleeding which are absent in the biomaterial excised after fixation.

of branch points seen in the vasculature within a given scaffold.

Statistical analysis

GraphPad Prism 7 was used to analyse data. Three scaffolds were analysed per sample tested, and the data are presented as mean ± standard error of the mean (SE). A non-parametric Kruskal–Wallis test was used to compare the differences in vascular density and bifurcation points for each biomaterial tested. A value of $p < 0.05$ was considered significant.

Results

CAM assay method optimisation

In this study, we modified and optimised the *ex ovo* CAM assay method previously reported in the literature using a glass-cling film set-up.[13,23,27] To increase the survival of the embryos in *ex ovo* conditions, we added AM solution on the developing CAM. Dohle et al.[13] reported an improved method of *ex ovo* cultures, which allows the survival of embryos to be over 50%. In our hands, using methods similar those reported by Dohle et al., we observed the survival rate to be ~44%. We further optimised their protocol by the addition of antimicrobial solution to prevent contamination and by using our proposed glass-cling film set-up to avoid trauma to the embryo. Using our proposed method, we repeatedly observed a significant improvement in the survival rate of embryos,

which repeatedly exceeded 60%. Therefore, we present a new approach to the traditional *ex ovo* CAM assays with improved embryo survival rates. Furthermore, for the excision of biomaterials from the CAM, we used a novel method of, first, cryotherapy and, second, fixation of the entire CAM using 4% PFA prior to excision of the scaffold. This prevented excessive bleeding from the surrounding vessels (Figure 4).

Biomaterial composition and structure

Using our proposed method, we examined a wide variety of biomaterials categorised as natural, synthetic, natural/synthetic and natural/natural polymers (Figure 5 and Table 1). The SEM images show the differences in the structure of the different biomaterials. Within every category of biomaterial composition tested, each biomaterial further represented a range of pore sizes referred to as the GPS (Figure 6). For example, macro-PCL has the majority of pores over 120 μm, in addition to the pores in the size range between 0 and 59 μm. Silicone (in the same category) showed the majority of pores to be between 20 and 39 μm, with pores also in the range of 0–19 μm and 60–79 μm. Only 6% of the pores were over 120 μm for elastin, with a majority in the 80–99 μm range (in the natural biomaterial category), whereas at least 21% of the pores in collagen (in the same category) were over 120 μm, with a majority in the range of 20–39 μm. The GPS is a consequence of the fabrication process of natural polymers, whereas for synthetic polymers such as PCL, electrospinning method was used, enabling
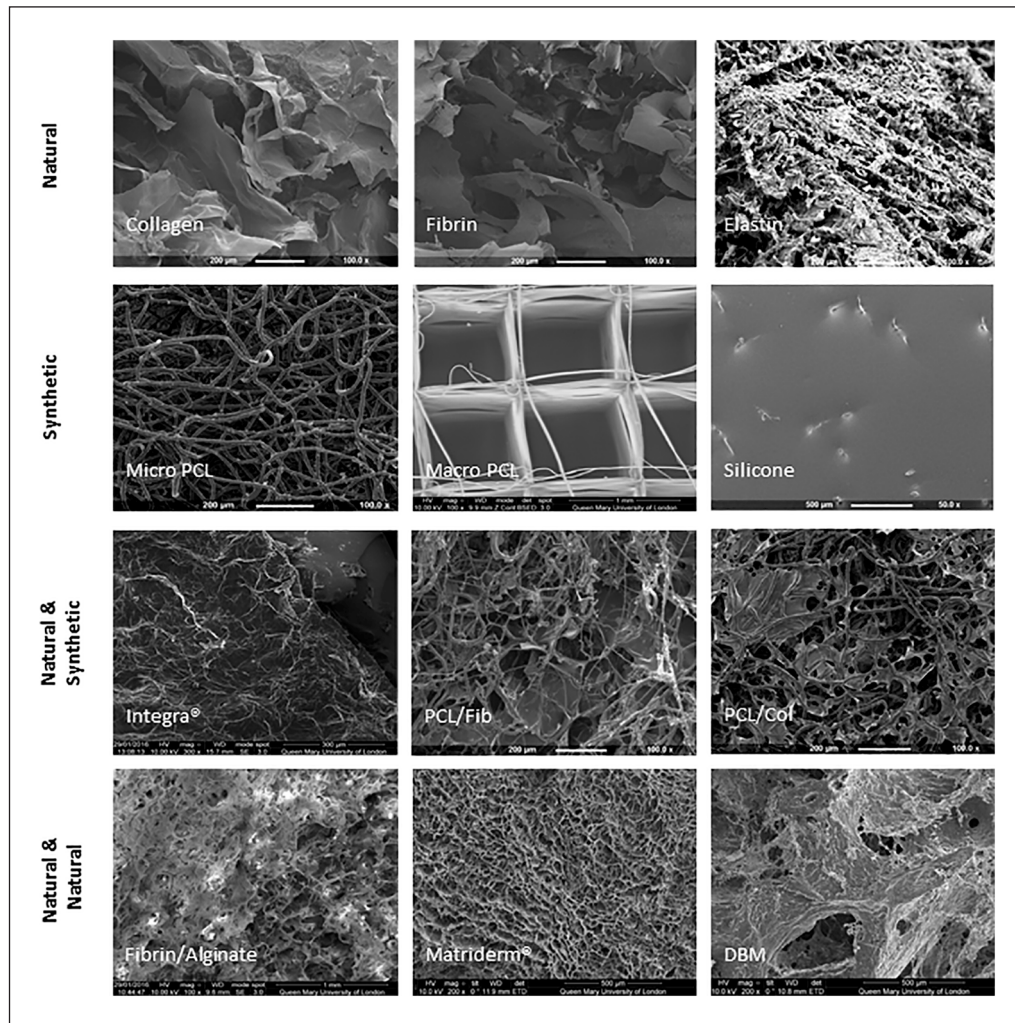
Figure 5. Representative SEM images of the biomaterials. The SEM results showed the structural variation in porosity, pore size and the general architecture of the scaffold.

a controllable pore size range. The overall porosity is an indicator of the total void space within a biomaterial. A variation in the overall porosity of biomaterials was observed (Table 2). The GPS, together with overall porosity, is an important indicator of the porous structure of the biomaterial.

Comparative angiogenic capacity of various biomaterials

The CAM assays showed varying degrees of blood vessel infiltration within the different biomaterials tested (Figure 7). Blood vessels penetrate from the edges of the biomaterial towards the centre of the biomaterial, and infiltration of vessels was noted throughout the depth of the biomaterial. Blood vessel infiltration was seen to a greater extent in VEGF-soaked discs (positive control) compared to PBS-soaked discs (negative control). Histology sections corroborated the observation that the

blood vessel infiltrated within the biomaterial (Figure 8). Blood vessels were observed in all the scaffolds tested except silicone where no blood vessels were seen to infiltrate the scaffold. In all the other biomaterials, vascularisation was seen at varying extents depending on the composition and porosity of the individual biomaterial.

The quantification of binary images allowed a more detailed comparison of the biomaterials (Figure 9). Fibrin, a pro-angiogenic protein,[31,32] had the highest amount of vascularisation as seen in the stereo microscopic images, either as a monomeric biomaterial (Fibrin) or as a composite, combined with either a natural (Fibrin/Alginate) or a synthetic polymer (PCL/Fib). Within the natural polymers, fibrin showed the highest amount of vascularisation and bifurcation points compared to collagen and elastin. However, these differences were only significant for vascular density between collagen and fibrin and not for elastin. For synthetic polymers, both macro- and micro-PCL showed similar vascular density;
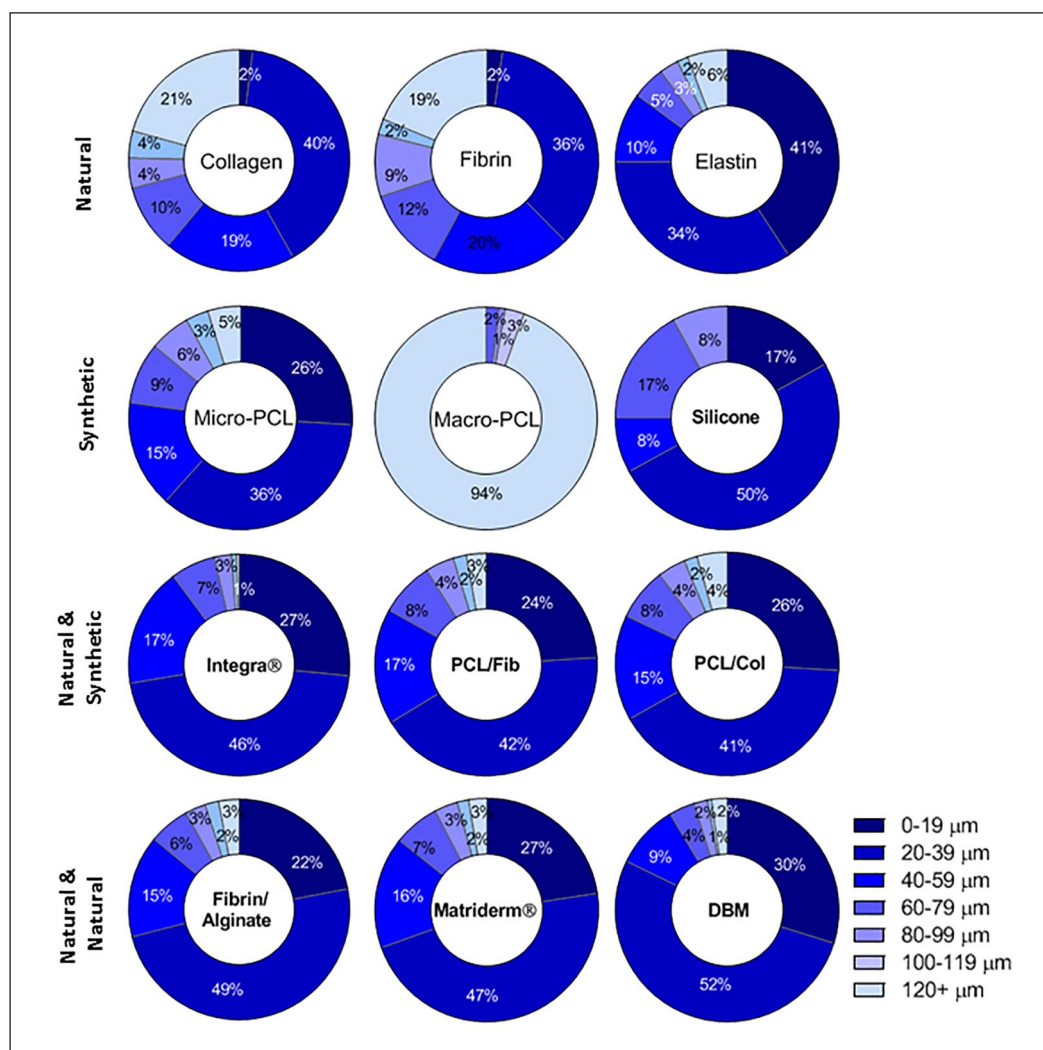
Figure 6. The GPS of the biomaterials tested. Doughnut-pie charts revealed a wide range of pore sizes within the biomaterials tested as indicated by the different colours. The lighter the colour, the greater the percentage of larger pores. All the biomaterials tested were composed of both micro-pores and macro-pores (pores over 100 µm).

Table 2. Percentage porosity of the biomaterials tested.

Composition category	Scaffold	Porosity (%)
Natural	Collagen	56.8 ± 2.08
	Fibrin	77.17 ± 1.19
	Elastin	33.54 ± 1.59
Synthetic	Micro-PCL	80.78 ± 0.92
	Macro-PCL	93.79 ± 0.94
	Silicone	2.98 ± 0.15
Natural/Synthetic	Integra®	90.02 ± 1.98[28]
	PCL/Fib	53.18 ± 0.56
	PCL/Col	57.64 ± 0.72
Natural/Natural	Fibrin/Alginate	76.39 ± 2.89[29]
	Matriderm®	90 ± 4.00
	DBM	62.24 ± 4.38[30]

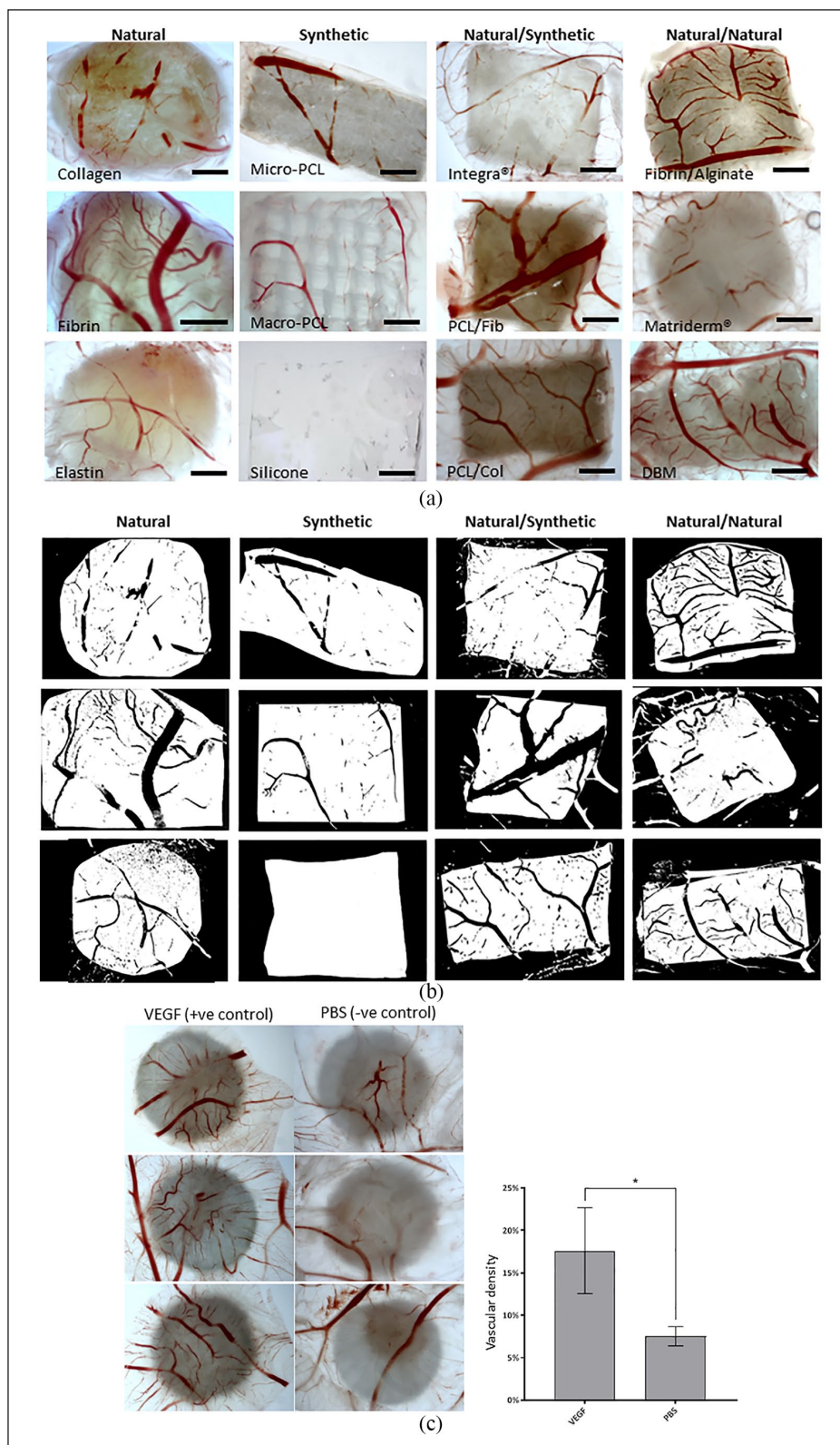DBM: demineralised bone matrix; PCL: poly-ε-caprolactone.

Figure 7. Representative stereo microscope and binary images of the biomaterials tested. (a) Differences were observed in the vascular infiltration of the different biomaterials tested as indicated by the growth of blood vessels (in red) within these biomaterials. It must be noted that these scaffolds were inverted, so the blood vessel infiltration is observed from the bottom of the biomaterial. Scale bar = 1 mm. (b) The edges of the biomaterial can be easily identified in the binary images where the scaffold itself is shown in white over a black background with blood vessels within the biomaterial shown in black. (c) Controls of VEGF-soaked (+ve) and PBS-soaked (–ve) filter discs showing differences in blood vessel infiltration, with positive control showing a significantly higher ($p = 0.02$; unpaired t-test) vascular density than the negative control. Data are presented as mean ± SE.
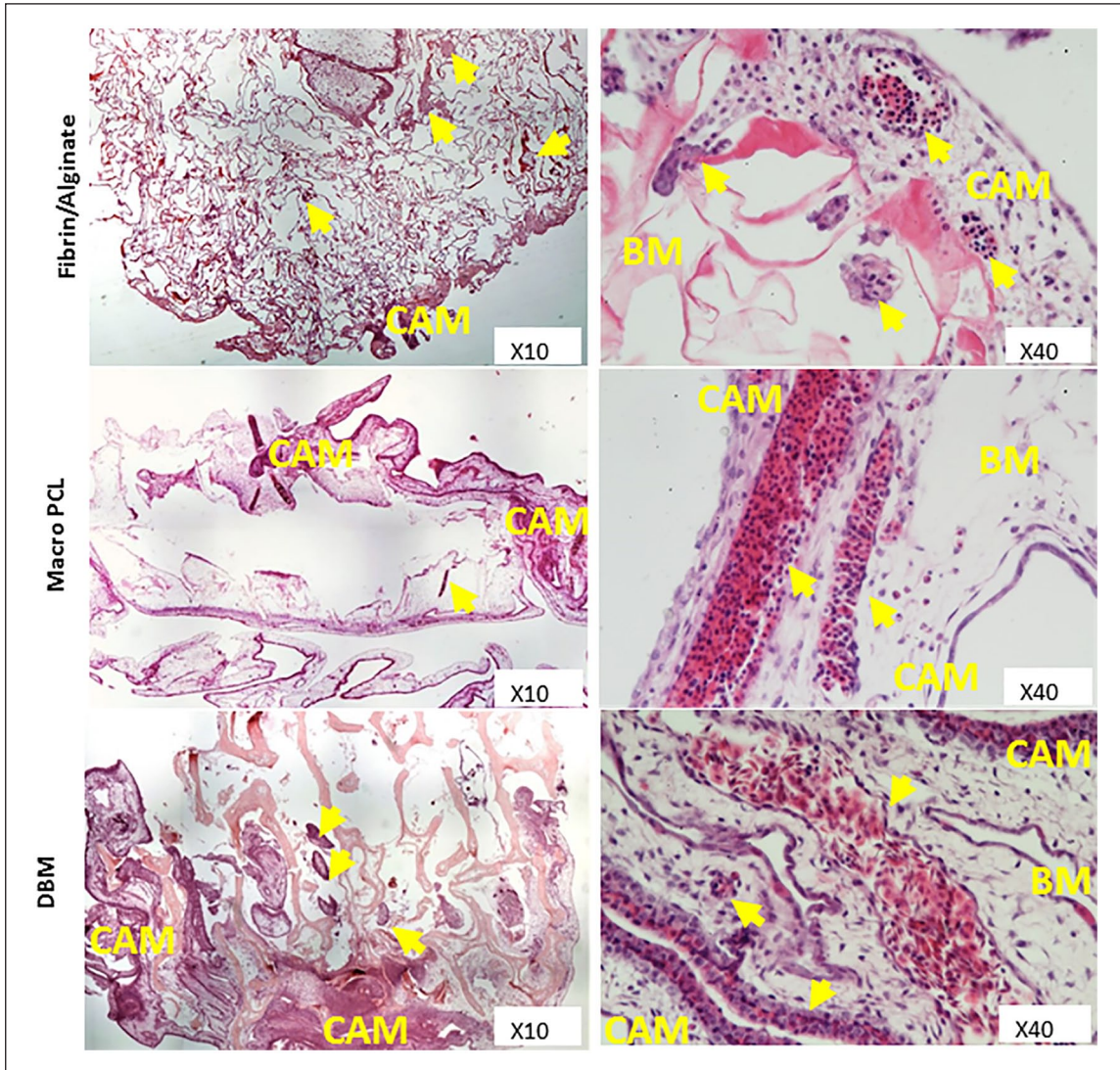
Figure 8. Representative H&E-stained images of biomaterials. The histology images show the presence of blood vessels within the biomaterial. Yellow arrows point to the blood vessels; CAM refers to the CAM tissue surrounding the biomaterial and BM refers to the biomaterial.

however, macro-PCL showed a greater number of bifurcation points. This may be due to the presence of many macro-pores, which allows the new capillaries to bifurcate more freely than in the micro-PCL scaffolds. This difference, however, was not significant. For the natural/synthetic composite biomaterials, PCL/Fib showed a greater vascular density compared to Integra®, although not significantly greater. Furthermore, PCL/Fib showed fewer bifurcation points than PCL/Col. The vessels within fibrin-based biomaterials appeared relatively thick compared to the vessels in other biomaterials, covering a large surface area, which could be due to the pro-angiogenic capacity of fibrin.[31,32] Fibrin/Alginate and DBM, within the natural/natural composite biomaterials, showed greater vascular density and bifurcation points compared to Matriderm®, although these differences

were only significant for bifurcation points. Individual significant differences for vascular density and bifurcation points are listed in Tables 3 and 4.

Discussion

The *ex ovo* method presented in this study is to the best of our knowledge the most optimised method for conducting CAM assays, with embryo survival rate exceeding 60%. Although in the early 1980s a study conducted by Dunn et al.[33] reported an embryo survival rate exceeding 80%, they used a highly sophisticated method limited by the need for significant expertise and complicated machinery in the lab to perform the experiments. Similarly, in 1974, Auerbach et al.[34] used the Petri dish method for *ex ovo* cultures; however, they reported a loss of 50% of the
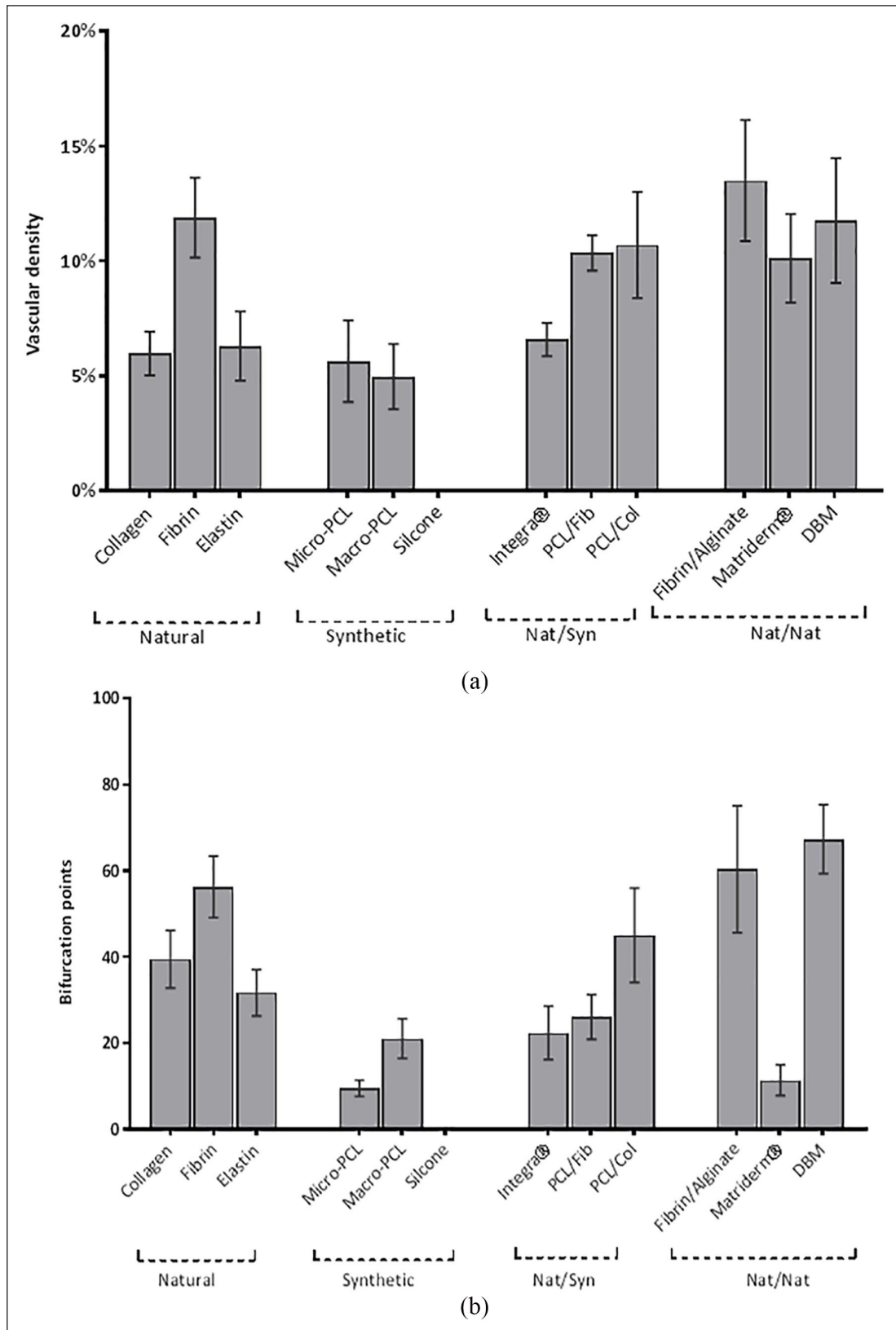
Figure 9. Vascular density and bifurcation points for each biomaterial. (a) Data for vascular density and bifurcation points corroborated the stereo microscope images. Overall, fibrin-based, monomeric or composite scaffolds showed better vascular infiltration than any other biomaterial. (b) Bifurcation point data showed a similar trend to vascular density data, with the exception of PCL/Fib and Matriderm® showing fewer bifurcation points. Data are presented as mean ± SE. Statistical significance of both graphs is listed in Tables 3 and 4.

Table 3. Statistically significant values for biomaterial vascular density.

Collagen vs Fibrin	*	0.0481
Collagen vs Fibrin/Alginate	*	0.0300
Fibrin vs Macro-PCL	*	0.0272
Fibrin vs Silicone	**	0.0019
Elastin vs Fibrin/Alginate	*	0.0439
Macro-PCL vs Fibrin/Alginate	*	0.0163
Micro-PCL vs Fibrin/Alginate	*	0.0330
Silicone vs PCL/Fib	**	0.0059
Silicone vs PCL/Col	**	0.0075
Silicone vs Fibrin/Alginate	***	0.0010
Silicone vs Matriderm®	**	0.0094
Silicone vs DBM	**	0.0047
Integra® vs Fibrin/Alginate	*	0.0481

DBM: demineralised bone matrix; PCL: poly-ε-caprolactone.
*$p < 0.05$; **$p < 0.01$; ***$p < 0.001$.

Table 4. Statistically significant values for biomaterial bifurcation points.

Collagen vs Silicone	*	0.0146
Fibrin vs Micro-PCL	**	0.0075
Fibrin vs Silicone	**	0.0013
Fibrin vs Matriderm®	*	0.0117
Elastin vs Silicone	*	0.0363
Macro-PCL vs DBM	*	0.0314
Micro-PCL vs PCL/Col	*	0.0346
Micro-PCL vs Fibrin/Alginate	**	0.0075
Micro-PCL vs DBM	**	0.0025
Silicone vs PCL/Col	**	0.0079
Silicone vs Fibrin/Alginate	**	0.0013
Silicone vs DBM	***	0.0004
Integra® vs DBM	*	0.0381
Fibrin/Alginate vs Matriderm®	*	0.0117
Matriderm® vs DBM	**	0.0041

DBM: demineralised bone matrix; PCL: poly-ε-caprolactone.
*$p < 0.05$; **$p < 0.01$; ***$p < 0.001$.

embryos in the first 3 days of incubation. Contamination post *ex ovo* is one of the main reasons for embryonic death in addition to trauma caused from the hard surface of the Petri dish. In our method, we use a simple glass-cling film set-up which can be easily replicated by other researchers, minimising trauma to the embryo. Furthermore, we used a crack open technique without the need for opening the egg using a jigsaw or cut-off wheel as previously reported.[21,27] A recent comprehensive study by Mangir et al.[23] also reported on a step-by-step protocol for conducting *ex ovo* CAM assays to assess a biomaterial's angiogenic response and biocompatibility. They used antibiotics in a weighing boat set-up and observed a survival rate of 68% by an intermediate user compared to over 80% by an experienced user. In our study, we did not compare antibiotic solution in a weighing boat set-up due to the trauma associated with the hard surface of the weighing boat compared to the soft cling film. Moreover, for a beginner using their method, the survival rates were around 25%, similar to what we observed in our labs. However, using our glass-cling film set-up, a new user in our lab was able to achieve a survival rate of over 60%. This method is safe, time-efficient and results in a higher survival rate of the embryos.

The second aim of this study was to further report the suitability of our optimised *ex ovo* method in the screening of biomaterials to select candidates for further development. We did this by testing the angiogenic properties (i.e. vascular density, number of bifurcation points and presence of blood vessels within the biomaterial) of a wide range of biomaterials intended for various hard and soft tissue applications using our *ex ovo* CAM method as a readout. The biomaterials used in this study differ in composition and structure, and therefore, a variety of angiogenic capacities would be expected. Data presented in this study did indeed show that a biomaterial's composition and structure can have a significant effect on its angiogenic capacity. Various studies have previously suggested

that the porous architecture of a biomaterial plays an important role in its revascularisation *in vivo*.[35–37] It has also been shown that the composition of the biomaterial will affect vascularisation *in vivo*.[38] However, there is currently no consensus about the best combination of biomaterial composition and porosity for successful angiogenesis *in vivo*. Previous studies have utilised *in ovo* and *ex ovo* CAM assays to examine angiogenesis and regenerative capacities of biomaterials such as hyaluronic acid–based scaffolds, silk fibroin scaffolds and other natural and synthetic polymers.[39–41] A study by Keshaw et al.[40] showed that using an *in ovo* CAM assay, a significant increase in blood vessel infiltration was seen in collagen spheres compared to PCL spheres. However, a major drawback of the *in ovo* studies is that it does not allow a direct comparison between multiple samples as only one sample can be placed on the CAM at a time. In our study, we were able to compare up to six different scaffolds on the same CAM.

In terms of the results observed, fibrin-based materials showed the best growth of blood vessels. This was expected as fibrin is known to be pro-angiogenic in nature.[31,32] PCL/Fib, however, showed a lower number of bifurcation points compared to fibrin/alginate, as well as fibrin on its own. Bifurcation points are reflective of the vessel sprouting phase of the angiogenesis process. During angiogenesis, pre-existing blood supply leads to vascular sprouting that subsequently develops into mature blood vessels. The sequential events that take place during angiogenesis are not fully understood, but it is generally believed that angiogenic sprouting occurs before mature vessel formation.[42] Therefore, it can be speculated that fibrin being pro-angiogenic leads to a rapid angiogenic response within these biomaterials where mature vessel formation was seen in all fibrin-based biomaterials as evident by the presence of thick vessels (Figure 3).

However, perhaps due to monomeric fibrin scaffold and fibrin/alginate scaffold constituting greater porosity than PCL/Fib, a greater number of bifurcation points were seen in the former two scaffolds. This suggests that while the biomaterial is composed of a pro-angiogenic protein, which encourages infiltration of blood vessels, it may not encourage further blood vessel sprouting due to the low porosity of the biomaterial. Our findings are consistent with previously published studies that suggest the presence of macro-pores and higher porosity is beneficial for the growth of blood vessels *in vivo*.[35,43,44] However, just having a higher porosity is insufficient for adequate angiogenesis. For instance, macro-PCL biomaterial used in this study constituted 87% of the pores in the macro-pore range with an overall porosity of $93.79 \pm 0.94\%$, yet showed poor angiogenic capacity which could be attributed to the polymeric composition, as PCL alone does not favour the growth of endothelial cells.[45] Similarly, Integra®, a commercially available clinical scaffold used for the treatment of full-thickness skin wounds, constituted an overall porosity of $90.02 \pm 1.98\%$, yet showed limited vascularisation. This may be, again, due to the composition of the biomaterial, particularly the glycosaminoglycan content in Integra®, which has been previously shown to inhibit angiogenesis.[46–48] *In vivo* studies[49,50] in mice have shown that Integra® exhibits between 3% and 17% blood vessel area, which is similar to the results reported using the *ex ovo* CAM method described in this study. Moreover, Integra® when combined with a fibrin sealant shows vascularity of over 20%.[50] These studies corroborate the finding presented in this article with increased angiogenesis seen in fibrin-based biomaterials.

The synthetic materials, in general, showed poor angiogenesis. It may be speculated that since synthetic materials lack the natural extracellular matrix (ECM) molecules, they would not encourage vascularisation. Previous studies have enhanced the ability of PCL scaffolds to encourage angiogenesis by coating with heparin and VEGF as well as combining PCL with other polymers.[51–53] It is also well established that synthetic biomaterials should be used in combination with the natural ECM molecules such as collagen and fibrin in order to enhance their regenerative potential,[54,55] with the exception of certain synthetic materials including bioactive bioglasses, which are known to stimulate angiogenesis *in vivo*.[56] From the data obtained in this study, it is difficult to warrant any further conclusions on synthetic scaffolds as the choice of the synthetic materials used in this study was quite limited, although both PCL and silicone are widely used for medical applications.[57,58] Further work needs to be conducted on a wider range of synthetic biomaterials to make further conclusions about their angiogenic capacity.

Adding a natural polymer (fibrin or collagen) to synthetic scaffolds significantly improved their ability to undergo vascularisation, even when the porosity remains lower than 70%.[43] Collagen and fibrin are the two key ECM molecules that have previously been shown to favour angiogenesis.[59–61] These findings suggest that when a biomaterial is composed of composites containing a pro-angiogenic material like fibrin or a natural ECM molecule like collagen type I, the porosity does not have a significant effect on the overall angiogenic capacity of the biomaterial so long as it allows vascular infiltration.

In conclusion, we utilised an optimised *ex ovo* CAM assay to screen a variety of biomaterials commonly used in tissue engineering and biomedical applications. From our results, the presented *ex ovo* CAM assay would be effective for pre-screening biomaterials prior to *in vivo* testing as evident by the variation observed in the angiogenic capacity of the 12 different biomaterials tested. However, further studies are required to confirm that the results are consistent with the *in vivo* situation. Furthermore, in-depth histological evaluation of a selected biomaterial after excision from the CAM could be performed to further evaluate the angiogenic response of the biomaterials after placement on the CAM. However, our study aimed at performing an initial screening of a variety of biomaterials to see whether our proposed method could detect differences between the materials tested, which our results showed it did. The angiogenic response observed on the CAM was as expected, with fibrin-based scaffolds showing the greatest amount of vascularisation. Furthermore, interesting interactions were observed when the effect of angiogenesis was attributed to the variation in porosity and composition. To the best of our knowledge, we are the first group to test such a large number of scaffolds on a very sensitive *ex ovo* angiogenesis assay. In conclusion, this study has demonstrated that a biomaterial's composition and porosity have a direct effect on its intrinsic angiogenic capacity, and this effect can be evaluated using an *ex ovo* CAM assay such as the one described here.

Data availability statement

Data generated and analysed during this study are included in this published article. Data and materials are available from the corresponding author subject to reasonable request and subject to the ethical approvals in place and material transfer agreements.

Declaration of conflicting interests

The author(s) declared the following potential conflicts of interest with respect to the research, authorship, and/or publication of this article: Dr Lilian Hook is the Chief Scientific Officer of Smart Matrix Limited (SML), while two of the authors, Dr Vaibhav Sharma and Dr Elena García-Gareta, provide services to SML, established to take the humanised version of fibrin/alginate dermal replacement scaffold through the development stage and

Research ethics

The research conducted in this study was as per the guidelines of the Institutional Animal Care and Use Committee (IACUC) and the National Institutes of Health (NIH), USA.

ORCID iD

Nupur Kohli 🔘 https://orcid.org/0000-0003-4216-1921

References

1. Stavropoulos A, Sculean A, Bosshardt DD, et al. Pre-clinical in vivo models for the screening of bone biomaterials for oral/craniofacial indications: focus on small-animal models. *Periodontol* 2015; 68(1): 55–65.
2. Trachtenberg JE, Vo TN and Mikos AG. Pre-clinical characterization of tissue engineering constructs for bone and cartilage regeneration. *Ann Biomed Eng* 2015; 43(3): 681–696.
3. Moreno-Jimenez I, Kanczler JM, Hulsart-Billstrom G, et al. The chorioallantoic membrane assay for biomaterial testing in tissue engineering: a short-term in vivo preclinical model. *Tissue Eng Part C* 2017; 23(12): 938–952.
4. Schlatter P, Konig MF, Karlsson LM, et al. Quantitative study of intussusceptive capillary growth in the chorioallantoic membrane (CAM) of the chicken embryo. *Microvasc Res* 1997; 54(1): 65–73.
5. Lafferty KJ and Jones MA. Reactions of the graft versus host (GVH) type. *Aust J Exp Biol Med Sci* 1969; 47(1): 17–54.
6. Baiguera S, Macchiarini P and Ribatti D. Chorioallantoic membrane for in vivo investigation of tissue-engineered construct biocompatibility. *J Biomed Mater Res B Appl Biomater* 2012; 100(5): 1425–1434.
7. FDA Wound Healing Clinical Focus Group. Guidance for industry: chronic cutaneous ulcer and burn wounds-developing products for treatment. *Wound Repair Regen* 2001;9(4): 258–268.
8. Kue CS, Tan KY, Lam ML, et al. Chick embryo chorioallantoic membrane (CAM): an alternative predictive model in acute toxicological studies for anti-cancer drugs. *Exp Anim* 2015; 64(2): 129–138.
9. Manjunathan R and Ragunathan M. Chicken chorioallantoic membrane as a reliable model to evaluate osteosarcoma – an experimental approach using SaOS2 cell line biological procedures online. *Biol Proced* 2015; 17: 10.
10. Zwadlo-Klarwasser G, Gorlitz K, Hafemann B, et al. The chorioallantoic membrane of the chick embryo as a simple model for the study of the angiogenic and inflammatory response to biomaterials. *J Mater Sci Mater Med* 2001; 12(3): 195–199.
11. Nguyen M, Shing Y and Folkman J. Quantitation of angiogenesis and antiangiogenesis in the chick embryo chorioallantoic membrane. *Microvasc Res* 1994; 47(1): 31–40.
12. Ponce ML, Kleinmann HK, Ponce ML, et al. The chick chorioallantoic membrane as an in vivo angiogenesis model. In: Bonifacino JS, Green KJ, Lippincott-Schwartz J, et al. (eds) *Current Protocols in Cell Biology*. Hoboken, NJ: John Wiley & Sons, pp. 19.5.1–19.5.6.
13. Dohle DS, Pasa SD, Gustmann S, et al. Chick ex ovo culture and ex ovo CAM assay: how it really works. *J Vis Exp* 2009(33): 1620.
14. Enrique Z and Frank C. *The textbook of angiogenesis and lymphangiogenesis: methods and applications*. Dordrecht: Springer.
15. Nuss KMR and von Rechenberg B. Biocompatibility issues with modern implants in bone – a review for clinical orthopedics. *Open Orthop J* 2008; 2: 66–78.
16. Anderson JM. Future challenges in the in vitro and in vivo evaluation of biomaterial biocompatibility. *Regen Biomater* 2016; 3(2): 73–77.
17. Scaglione S, Cilli M, Fiorini M, et al. Differences in chemical composition and internal structure influence systemic host response to implants of biomaterials. *Int J Artif Organs* 2011; 34(5): 422–431.
18. Oates M, Chen R, Duncan M, et al. The angiogenic potential of three-dimensional open porous synthetic matrix materials. *Biomaterials* 2007; 28(25): 3679–3686.
19. Steffens GCM, Yao C, Prevel P, et al. Modulation of angiogenic potential of collagen matrices by covalent incorporation of heparin and loading with vascular endothelial growth factor. *Tissue Eng* 2004; 10(9–10): 1502–1509.
20. Yao C, Markowicz M, Pallua N, et al. The effect of cross-linking of collagen matrices on their angiogenic capability. *Biomaterials* 2008; 29(1): 66–74.
21. Zijlstra A and Lewis DJ. Visualization and quantification of De Novo angiogenesis in ex ovo chicken embryos. In: Zudaire E, Cuttitta F (eds) *The textbook of angiogenesis and lymphangiogenesis: methods and applications*. Dordrecht: Springer, 2012, pp. 217–240.
22. Deryugina EI and Quigley JP. Chapter 2. Chick embryo chorioallantoic membrane models to quantify angiogenesis induced by inflammatory and tumor cells or purified effector molecules. *Method Enzymol* 2008; 444: 21–41.
23. Mangir N, Dikici S, Claeyssens F, et al. Using ex Ovo chick chorioallantoic membrane (CAM) assay to evaluate the biocompatibility and angiogenic response to biomaterials. *ACS Biomater Sci Eng* 2019; 5: 3190–3200.
24. Ristovski N, Bock N, Liao S, et al. Improved fabrication of melt electrospun tissue engineering scaffolds using direct writing and advanced electric field control. *Biointerphases* 2015; 10(1): 011006.
25. National Institutes of Health. The public health service responds to commonly asked questions. *ILAR News* 1991; 33(4): 68–70.
26. An Association of New England Medical Center Tufts. IACUC policy on protocol approval for use of chicken embryos and eggs, https://www.bu.edu/researchsupport/forms-policies/iacuc-use-of-live-embryonated-eggs-of-egg-laying-vertebrate-species/ (2001, accessed 10 June 2019).
27. Schomann T, Qunneis F, Widera D, et al. Improved method for ex ovo-cultivation of developing chicken embryos for

human stem cell xenografts. *Stem Cells Int* 2013; 2013: 960958.

28. Sharma V, Kohli N, Moulding D, et al. Design of a novel two-component hybrid dermal scaffold for the treatment of pressure sores. *Macromol Biosci* 2017; 17(11): 0185.

29. Sharma V, Patel N, Kohli N, et al. Viscoelastic, physical, and bio-degradable properties of dermal scaffolds and related cell behaviour. *Biomed Mater* 2016; 11(5): 055001.

30. Liu G, Sun J, Li Y, et al. Evaluation of partially demineralized osteoporotic cancellous bone matrix combined with human bone marrow stromal cells for tissue engineering: an in vitro and in vivo study. *Calcif Tissue Int* 2008; 83(3): 176–185.

31. Bootle-Wilbraham CA, Tazzyman S, Thompson WD, et al. Fibrin fragment E stimulates the proliferation, migration and differentiation of human microvascular endothelial cells in vitro. *Angiogenesis* 2001; 4(4): 269–275.

32. Thomson KS, Dupras SK, Murry CE, et al. Proangiogenic microtemplated fibrin scaffolds containing aprotinin promote improved wound healing responses. *Angiogenesis* 2014; 17(1): 195–205.

33. Dunn BE, Fitzharris TP and Barnett BD. Effects of varying chamber construction and embryo pre-incubation age on survival and growth of chick embryos in shell-less culture. *Anat Rec* 1981; 199(1): 33–43.

34. Auerbach R, Kubai L, Knighton D, et al. A simple procedure for the long-term cultivation of chicken embryos. *Dev Biol* 1974; 41(2): 391–394.

35. Feng B, Jinkang Z, Zhen W, et al. The effect of pore size on tissue ingrowth and neovascularization in porous bioceramics of controlled architecture in vivo. *Biomed Mater* 2011; 6(1): 015007.

36. Lu JX, Flautre B, Anselme K, et al. Role of interconnections in porous bioceramics on bone recolonization in vitro and in vivo. *J Mater Sci Mater Med* 1999; 10(2): 111–120.

37. Mastrogiacomo M, Scaglione S, Martinetti R, et al. Role of scaffold internal structure on in vivo bone formation in macroporous calcium phosphate bioceramics. *Biomaterials* 2006; 27(17): 3230–3237.

38. Moon JJ and West JL. Vascularization of engineered tissues: approaches to promote angio-genesis in biomaterials. *Curr Top Med Chem* 2008; 8(4): 300–310.

39. Cirligeriu L, Cimpean A, Calniceanu H, et al. Hyaluronic acid/bone substitute complex implanted on chick embryo chorioallantoic membrane induces osteoblastic differentiation and angiogenesis, but not Inflammation. *Int J Mol Sci* 2018; 19: 4119.

40. Keshaw H, Thapar N, Burns AJ, et al. Microporous collagen spheres produced via thermally induced phase separation for tissue regeneration. *Acta Biomater* 2010; 6(3): 1158–1166.

41. Valdes TI, Kreutzer D and Moussy F. The chick chorioallantoic membrane as a novel in vivo model for the testing of biomaterials. *J Biomed Mater Res* 2002; 62(2): 273–282.

42. Irvin MW, Zijlstra A, Wikswo JP, et al. Techniques and assays for the study of angiogenesis. *Exp Biol Med* 2014; 239(11): 1476–1488.

43. Chen Y, Wang J, Zhu X, et al. The directional migration and differentiation of mesenchymal stem cells toward vascular endothelial cells stimulated by biphasic calcium phosphate ceramic. *Regen Biomater* 2018; 5: 129–139.

44. Karageorgiou V and Kaplan D. Porosity of 3D biomaterial scaffolds and osteogenesis. *Biomaterials* 2005; 26(27): 5474–5491.

45. Pankajakshan D, Krishnan VK and Krishnan LK. Vascular tissue generation in response to signaling molecules integrated with a novel poly(ε-caprolactone)–fibrin hybrid scaffold. *J Tissue Eng Regen Med* 2007; 1: 389–397.

46. Liang JH and Wong KP. *The characterization of angiogenesis inhibitor from shark cartilage*. Boston, MA: Springer, pp. 209–223.

47. De Rossi G, Evans AR, Kay E, et al. Shed syndecan-2 inhibits angiogenesis. *J Cell Sci* 2014; 127(Pt. 21): 4788–4799.

48. Kobayashi T, Kakizaki I, Nozaka H, et al. Chondroitin sulfate proteoglycans from salmon nasal cartilage inhibit angiogenesis. *Biochem Biophys Rep* 2017; 9: 72–78.

49. Frueh FS, Spater T, Korbel C, et al. Prevascularization of dermal substitutes with adipose tissue-derived microvascular fragments enhances early skin grafting. *Sci Rep* 2018; 8(1): 10977.

50. Wilcke I, Lohmeyer JA, Liu S, et al. VEGF165 and bFGF protein-based therapy in a slow release system to improve angiogenesis in a bioartificial dermal substitute in vitro and in vivo. *Langenbeck's Arch Surg* 2007; 392: 305–314.

51. Serbo JV and Gerecht S. Vascular tissue engineering: biodegradable scaffold platforms to promote angiogenesis. *Stem Cell Res Ther* 2013; 4(1): 8.

52. Zhang WJ, Liu W, Cui L, et al. Tissue engineering of blood vessel. *J Cell Mol Med* 2007; 11: 945–957.

53. Singh S, Wu BM and Dunn JCY. Accelerating vascularization in polycaprolactone scaffolds by endothelial progenitor cells. *Tissue Eng Part A* 2011; 17(13–14): 1819–1830.

54. IkoneN L. Analysis of different natural and synthetic biomaterials to support cardiomyocyte growth. *J Clin Exp Cardiolog* 2013; 04: 7.

55. Lutolf MP and Hubbell JA. Synthetic biomaterials as instructive extracellular microenvironments for morphogenesis in tissue engineering. *Nat Biotechnol* 2005; 23(1): 47–55.

56. Baino F, Hamzehlou S and Kargozar S. Bioactive glasses: where are we and where are we going? *J Funct Biomater* 2018; 9: 25.

57. Malikmmammadov E, Tanir TE, Kiziltay A, et al. PCL and PCL-based materials in biomedical applications. *J Biomater Sci Polym Ed* 2018; 29(7–9): 863–893.

58. Curtis J and Colas A. Medical applications of silicones. *Biomater Sci* 2013; 18: 1106–1116.

59. Feng X, Tonnesen MG, Mousa SA, et al. Fibrin and collagen differentially but synergistically regulate sprout angiogenesis of human dermal microvascular endothelial cells in 3-dimensional matrix. *Int J Cell Biol* 2013; 2013: 231279.

60. Hadjipanayi E, Kuhn P-H, Moog P, et al. The fibrin matrix regulates angiogenic responses within the hemostatic microenvironment through biochemical control. *PLoS ONE* 2015; 10(8): e0135618.

61. Rioja AY, Tiruvannamalai Annamalai R, Paris S, et al. Endothelial sprouting and network formation in collagen- and fibrin-based modular microbeads. *Acta Biomater* 2016; 29: 33–41.